

Resistance peak at the resistive transition in high- T_c superconductors

Minoru Suzuki

NTT Interdisciplinary Research Laboratories, Nippon Telegraph and Telephone Corporation, 162 Tokai, Ibaraki 319-11, Japan

(Received 26 October 1993; revised manuscript received 31 May 1994)

The resistance peak, which is occasionally observed near the resistive transition in high- T_c superconductors, is shown by numerical analysis to arise from a slight inclination of the sample face from the CuO_2 planes. This inclination combined with large conductivity anisotropy causes a significant distribution of the current density and reduces the voltage drop between voltage probes, resulting in a very small apparent resistivity and high residual resistivity ratio. In the resistive transition region, on the other hand, the anisotropy abruptly decreases, and the apparent resistance increases and approaches the true value before the resistivity vanishes, resulting in an apparent peak. The resistance peak is therefore a manifestation of the fact that the resistive transition along the c axis is much sharper than that in the CuO_2 planes.

I. INTRODUCTION

The resistance peak (RP) at the superconducting transition has long been a puzzle. Even recently, a sharp RP very close to the superconducting transition was observed by Crusellas, Fontcuberta, and Piñol¹ in a single crystal of $\text{Nd}_{2-x}\text{Ce}_x\text{CuO}_{4-\delta}$. They argued that this phenomenon might be explained by reentrant superconductivity associated with some granular superconductivity. More recently, Wan *et al.*² observed a voltage peak (or a RP if divided by current) in a $\text{Bi}_2\text{Sr}_2\text{CaCu}_2\text{O}_{8-y}$ crystal. They suggested that it might be caused by the competition between the free-vortex dissipation due to thermal fluctuation and the interlayer Josephson coupling below T_c . Generally, however, this phenomenon is not reproducible and depends on the samples. Indeed, many crystals show quite normal resistive transitions.

This phenomenon itself is not a novel one.³ Similar phenomena have been observed in $\text{Nd}_{2-x}\text{Ce}_x\text{CuO}_{4-\delta}$ crystals,⁴ $\text{La}_{2-x}\text{Sr}_x\text{CuO}_4$ crystals,⁵ $\text{YBa}_2\text{Cu}_3\text{O}_{7-y}$ crystals,⁶ epitaxial thin films of $\text{Nd}_{2-x}\text{Ce}_x\text{CuO}_{4-\delta}$ and $\text{La}_{2-x}\text{Sr}_x\text{CuO}_4$, as described later, $\text{YBa}_2\text{Cu}_3\text{O}_{7-y}$ epitaxial films,⁷ and even in TaSe_3 crystals⁸ and multilayer thin films.^{9,10} Although the physics of this phenomenon has been described in various ways, no definite interpretation has yet been presented.

In this paper, a simple model is proposed which provides a definite explanation of this phenomenon. The model requires that the system has very large conductivity anisotropy. It is shown based on this model that the RP close to the resistive transition can be explained to result from a particular configuration of sample shape with respect to the CuO_2 planes in high- T_c superconductors (or highly conducting planes in other systems). This model for the RP is substantiated by numerical analysis. As a consequence of this interpretation, it is concluded that the RP is a manifestation of the fact that the resistive transition along the c axis occurs much faster than that in the CuO_2 planes.

II. RESISTANCE PEAK IN (103) EPITAXIAL FILMS OF

$\text{La}_{1.85}\text{Sr}_{0.15}\text{CuO}_4$ AND $\text{Nd}_{1.85}\text{Ce}_{0.15}\text{CuO}_{4-\delta}$

Before describing the model designed to explain the RP, typical RP experimental results are presented as a brief introduction to this phenomenon. Figures 1(a) and 1(b) show representative temperature dependence of resistivity $\rho(T)$ for a (103) $\text{La}_{1.85}\text{Sr}_{0.15}\text{CuO}_4$ epitaxial film in the $[30\bar{1}]$ and $[010]$ directions, respectively.¹¹ These characteristics are quite normal in that they are similar to those of bulk crystals.¹² However, when ρ in the CuO_2 planes is measured for (103) epitaxial films of $\text{La}_{1.85}\text{Sr}_{0.15}\text{CuO}_4$ or $\text{Nd}_{1.85}\text{Ce}_{0.15}\text{CuO}_{4-\delta}$ in the $[010]$ direction (more precisely, very close to the $[010]$ direction), $\rho(T)$ occasionally exhibits a RP such as that shown, for example, in Fig. 1(c) or Fig. 2.

In the case of Fig. 1, three samples were cut from the same wafer for the measurements of $\rho(T)$ in the $[010]$ direction [$\rho_{[010]}(T)$]. The pattern for two of the samples was made so that the pattern edge was precisely parallel to the CuO_2 planes, while the pattern of the other sample had an inclination of a few degrees (not specified) with respect to the CuO_2 planes. The first two samples exhibited nearly the same characteristics as in Fig. 1(b). The other exhibited the characteristics shown in Fig. 1(c). Although the samples were cut from positions within 5 mm of each other, the characteristic shown in Fig. 1(c) is totally different in quality. Since $\rho_{[010]}(T)$ is the resistivity in the CuO_2 planes (ρ_{ab}), $\rho_{[010]}(T)$ should behave similarly to $\rho_{ab}(T)$ measured for (001) epitaxial films.¹³ However, the characteristics in Fig. 1(c) have never been observed for (001) epitaxial films.

Some of the earlier works on the RP indicates that its height strongly depends on an applied magnetic field or applied current density. In the present case, however, there is no strong field dependence. Moreover, the shape of the RP depends only slightly on the applied current. Thus the field and current dependence behave differently for different samples. These facts force us to accept that

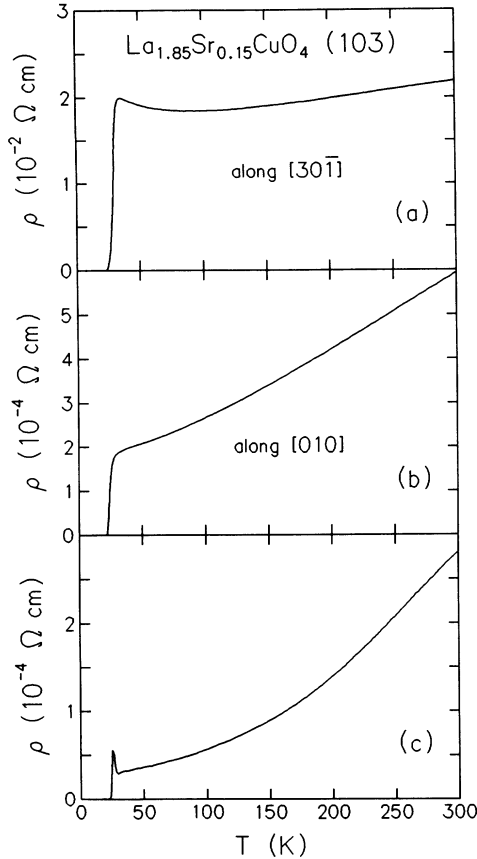


FIG. 1. Temperature dependence of resistivity $\rho(T)$ for $\text{La}_{1.85}\text{Sr}_{0.15}\text{CuO}_4$ (103) epitaxial thin films. These samples were cut from a single homogeneous thin film. (a) $\rho(T)$ along $[30\bar{1}]$, (b) $\rho(T)$ along $[010]$, (c) $\rho(T)$ in a direction inclined a few degrees from $[010]$.

this kind of phenomenon arises from a sample misalignment which leads to the inhomogeneous distribution of current density and potential when the sample is made of a system with very large conductivity anisotropy.

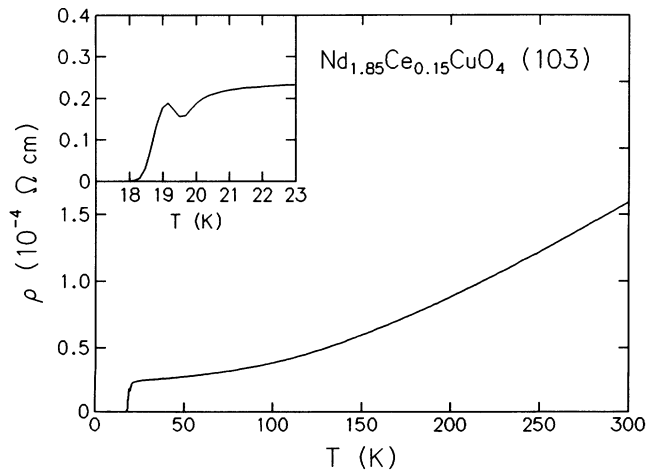


FIG. 2. Temperature dependence of resistivity $\rho(T)$ for a $\text{Nd}_{1.85}\text{Ce}_{0.15}\text{CuO}_{4-\delta}$ (103) epitaxial thin film in a direction close to $[010]$, showing the eventually observed RP.

III. MODEL FOR NUMERICAL ANALYSIS

First, we assume that samples are cut from a single-crystalline (100) epitaxial film (or a crystal). [The actual samples were cut from (103) epitaxial films, but this assumption makes analysis significantly simpler by reducing the problem to a two-dimensional one without affecting essential points.] Also we assume that the system under consideration has very large conductivity anisotropy. The other assumption is that there is a small angle θ between the CuO_2 planes and the sample face, as shown in the inset of Fig. 4 below. This last assumption is essential and a prerequisite to the following analysis. It should be noticed that this situation can commonly occur and causes the RP at the transition as shown in the following.

Within the framework of this model, we first calculate the potential distribution $V(x,y)$ in the sample. Let \mathbf{J} and \mathbf{E} be the current density and the electric field, respectively. Then \mathbf{J} is expressed by the equation

$$\mathbf{J} = \begin{bmatrix} \cos\theta & -\sin\theta \\ \sin\theta & \cos\theta \end{bmatrix} \hat{\sigma} \begin{bmatrix} \cos\theta & \sin\theta \\ -\sin\theta & \cos\theta \end{bmatrix} \mathbf{E},$$

$$\hat{\sigma} = \begin{bmatrix} \sigma_{\perp} & 0 \\ 0 & \sigma_{\parallel} \end{bmatrix},$$

where σ_{\parallel} and σ_{\perp} are conductivities parallel and perpendicular to the CuO_2 planes, respectively, and $\hat{\sigma}$ is a conductivity tensor. Since $\text{div } \mathbf{J} = 0$ within the sample, we obtain the expression

$$\begin{aligned} & [\sigma_{\perp} \cos^2\theta + \sigma_{\parallel} \sin^2\theta] \frac{dE_x}{dx} + (\sigma_{\perp} - \sigma_{\parallel}) \sin\theta \cos\theta \frac{dE_y}{dx} \\ & + (\sigma_{\perp} - \sigma_{\parallel}) \sin\theta \cos\theta \frac{dE_x}{dy} \\ & + [\sigma_{\perp} \sin^2\theta + \sigma_{\parallel} \cos^2\theta] \frac{dE_y}{dy} = 0. \end{aligned} \quad (1)$$

To simplify Eq. (1), we use new parameters defined by the relations

$$\begin{aligned} \alpha &= S \cos^2\theta + \sin^2\theta, \\ \beta &= (S - 1) \sin\theta \cos\theta, \\ \gamma &= S \sin^2\theta + \cos^2\theta, \end{aligned}$$

where $S^{-1} = \sigma_{\parallel} / \sigma_{\perp}$ is the anisotropy ratio of the conductivity. Then we obtain

$$\alpha \frac{d^2V}{dx^2} + 2\beta \frac{d^2V}{dy dx} + \gamma \frac{d^2V}{dy^2} = 0. \quad (2)$$

The boundary conditions for the numerical analysis are

$$V(x,0) = V \quad \text{and} \quad V(x,L) = 0, \quad (3)$$

and

$$\begin{aligned} \alpha \frac{dV(0,y)}{dx} + \beta \frac{dV(0,y)}{dy} &= 0, \\ \alpha \frac{dV(W,y)}{dx} + \beta \frac{dV(W,y)}{dy} &= 0, \end{aligned} \quad (4)$$

since $J_x(0,y)=J_x(W,y)=0$. Here, W and L indicate the width and the length of the sample. Thus the numerical analysis provides the potential distribution of a sample as a function of conductivity anisotropy ratio S and θ

Equations (2)–(4) are used to obtain values for $V(x,y)$ by numerical calculation for various sets of S and θ . Typical results are shown in Figs. 3(a) and 3(b) for $S^{-1}=25$ and $S^{-1}=400$ at $\theta=10^\circ$. The current distributions $J(x,y)$ corresponding to Figs. 3(a) and 3(b) are also shown in Figs. 3(c) and 3(d), where it is clearly seen that almost no current flows in the vicinity of the lateral faces. Here, it should be noticed that the anisotropy ratio of $S^{-1}=400$ is actually observed for $\text{Nd}_{2-x}\text{Ce}_x\text{CuO}_{4-\delta}$ and $\text{La}_{2-x}\text{Sr}_x\text{CuO}_4$, and the value of $S^{-1}=25$ roughly corresponds to that of $\text{YBa}_2\text{Cu}_3\text{O}_{7-y}$. For the Bi-Sr-Ca-Cu-O system, S^{-1} is much larger than 1000. Thus the inhomogeneous current and potential distribution seen in Fig. 3 is quite likely to occur in actually high- T_c superconductors. In Fig. 3, it is clearly seen that a slight angle misalignment causes a significant inhomogeneous distribution for $V(x,y)$ and $J(x,y)$, especially near the edges. Due to this inhomogeneous current distribution, the voltage drop V_{obs} between the voltage probes positioned inside the current electrodes (Fig. 4, inset below) decreases significantly. This is because most of the current flows through the path that has the least resistance and the

current density near the voltage probes becomes extremely small, as clearly seen in Figs. 3(c) and 3(d). Thus the voltage drop between the voltage probes V_{obs} becomes much smaller than the voltage V_0 , which is expected when $\theta=0$. That is, V_{obs} is a very sensitive function of θ and S^{-1} . When such inhomogeneous current distribution is established, the apparent resistivity ($\propto V_{\text{obs}}/I$) decreases significantly. In some cases, this effect leads to an extraordinarily large residual resistivity ratio, as seen in Fig. 1(c), compared to that observed in samples of an identical system exhibiting no RP.

For the numerical analysis of the RP, we placed the voltage probes at points $(W,0.1L)$ and $(W,0.9L)$, so that

$$\begin{aligned} V_{\text{obs}} &\equiv V(W,0.1L) - V(W,0.9L) \\ &= V(0,0.1L) - V(0,0.9L) . \end{aligned}$$

In the conventional four-probe method, we assume homogeneous current density, which is attained either when $\theta=0$ or when the medium extends to $\pm\infty$ in the x direction. In this case,

$$V(x,0.1L) - V(x,0.9L) = V_{\text{obs}}(\theta=0) = V_0 = 0.8V ,$$

i.e., $V_{\text{obs}}/V_0=1$ when $\theta=0$, and the value for V_0/I gives an accurate estimate for the resistance, where I is the applied current. In the present case, however, the observed

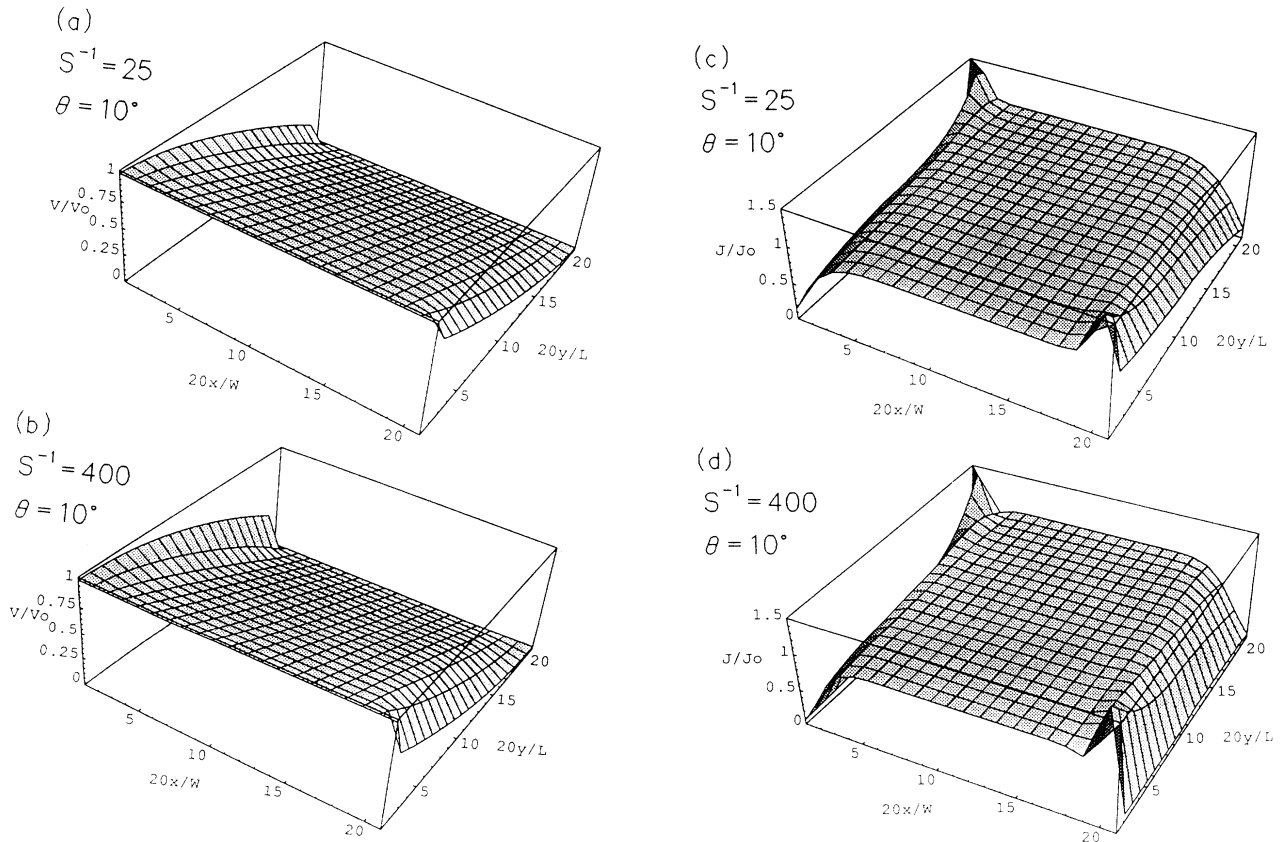


FIG. 3. Typical results of the numerical calculation of the potential $V(x,y)$ and current density distribution. (a) $V(x,y)/V$ when $S^{-1}=25$ and $\theta=10^\circ$, (b) $V(x,y)/V$ when $S^{-1}=400$ and $\theta=10^\circ$, (c) $J(x,y)$ when $S^{-1}=25$ and $\theta=10^\circ$, and (d) $J(x,y)$ when $S^{-1}=400$ and $\theta=10^\circ$. The values for $J(x,y)$ are normalized by the corresponding value when $\theta=0$.

voltage drop V_{obs} is markedly smaller than V_0 , and the resistance R is seriously underestimated when we use the conventional relation $R = V_{\text{obs}}/I$. Figure 4 shows the ratio of the voltage drop V_{obs} normalized by V_0 as a function of θ . Here, V_{obs}/V_0 is also the ratio of the underestimated R to the correct value. When the anisotropy S^{-1} is very large, V_{obs}/V_0 decreases to below 0.5 near $\theta=3^\circ$, where V_{obs}/V_0 reaches its minimum value. (It seems that the problem is that this phenomenon occurs when θ is very small.) When S^{-1} has a moderate value, V_{obs}/V_0 is around 0.9 and the effect is not significant. In the present analysis, we assume perfect electrodes with zero contact resistance. However, in an actual case, the electrodes have finite contact resistance as well as their own intrinsic resistance. This further enhances the inhomogeneous distribution, and V_{obs}/V_0 is expected to decrease drastically, leading to a serious underestimate of ρ .

The RP at the resistive transition is a consequence of this inhomogeneous current distribution. As long as the anisotropy ratio S^{-1} remains almost constant over the T range under study, no peak appears within the framework of the present model. However, this is not necessarily the case in the resistive transition region. If the resistive transition for ρ_c is much sharper than that for ρ_{ab} , S^{-1} decreases abruptly in the transition region. Then V_{obs}/V_0 increases to ≈ 1 and the apparent resistance increases to a value very close to the true one. At the end of the resistive transition, the true resistance itself becomes very small and vanishes. The whole sequence leads to the appearance of a RP in the transition region. This interpretation is substantiated by the fact that the T range for the resistive transition in Fig. 1 in both the [010] and [30 $\bar{1}$] directions nearly coincides with the T range for the RP.

The RP can be calculated numerically for a given value of θ by using the data for ρ_c ($=1/\sigma_{\perp}$) and ρ_{ab}

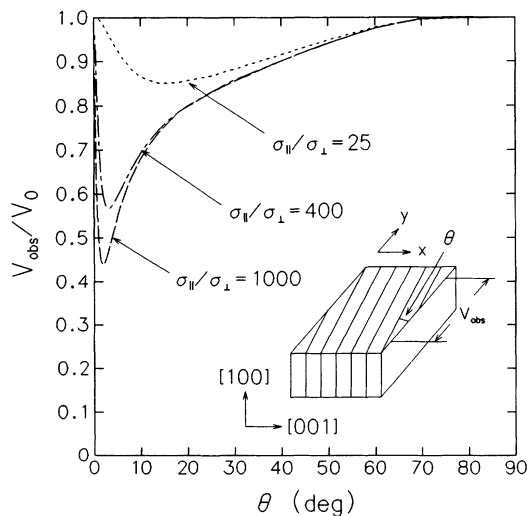


FIG. 4. Angular dependence of the apparent resistance (voltage drop V_{obs}/V_0), showing that the voltage drop decreases drastically due to a slight inclination of the sample edge from the CuO_2 planes. The inset shows a schematic representation of a sample configuration with respect to the CuO_2 planes.

($=1/\sigma_{\parallel}$). The values for $S^{-1}(T) = \rho_c(T)/\rho_{ab}(T)$ are obtained from the data in Figs. 1(a) and 1(b) using the relation

$$\rho_{[30\bar{1}]} = \rho_c \sin^2 \phi + \rho_{ab} \cos^2 \phi,$$

where $\phi = 49.34^\circ$ is the angle between the CuO_2 planes and the (103) plane. In this evaluation, it is assumed that $\rho_{ab}(T) = \rho_{[010]}(T)$. This is reasonable when it is taken into account that $\rho_{[010]}(T)$ in Fig. 1(b) is almost identical to $\rho_{ab}(T)$ observed for (001) epitaxial thin films.¹³ Figure 5 plots the numerical results for the apparent resistivity $\rho_{[010]}(T)/V_0(T)$ when $\theta = 3^\circ$. The calculated values are larger than the observed values by a factor of 2. This is probably due to the effect of the finite contact resistance. Except for this quantitative deviation, the numerical analysis shows that the present model explains the RP behavior quite well. As inferred from Fig. 4, the value of $\theta = 3^\circ$ gives a minimum for V_{obs}/V_0 when $S^{-1} = 400$, causing a pronounced RP. When θ increases or decreases from this value, the nonuniform current becomes less pronounced and the RP becomes smaller. The positioning of the voltage probes gives only a small change in the RP except for the vicinity of the current probes, since the drastic nonuniformity of the potential distribution is seen near the current probes.

Figure 6 shows the plots for $\rho_c(T)$ and $S^{-1}(T) = \rho_c(T)/\rho_{ab}(T)$ calculated from $\rho_{[010]}$ and $\rho_{[30\bar{1}]}$ in Fig. 1 using the above relation. The sharp drop in $S^{-1}(T)$ below ~ 30 K provides experimental evidence for the abrupt decrease in the conductivity anisotropy in the resistive transition region. This abrupt decrease in $S^{-1}(T)$ almost coincides with the onset of the transition in ρ_c , which is quite consistent with the present model and strongly indicates that $S^{-1}(T)$ is reflected by the

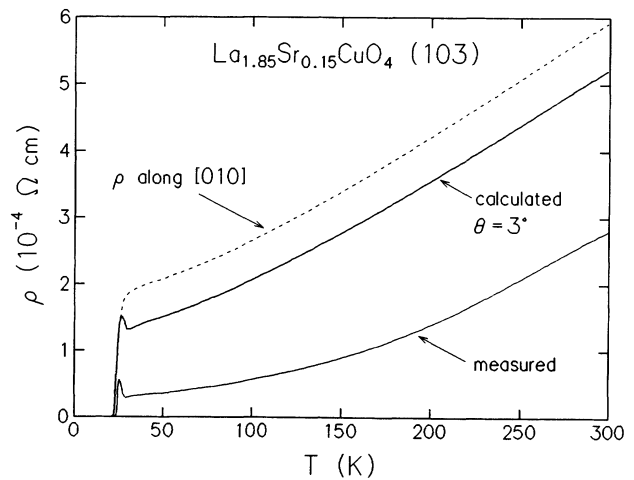


FIG. 5. Numerical calculation (thick solid line) of the apparent resistance when $\theta = 3^\circ$, using the data in Figs. 1(a) and 1(b). The dashed line is $\rho_{[010]}$ in Fig. 1(b). The thin solid line shows the experimental results. The numerical analysis produces a RP in the resistive transition region, indicating that the present model explains this phenomenon quite well in a totally different way from earlier studies.

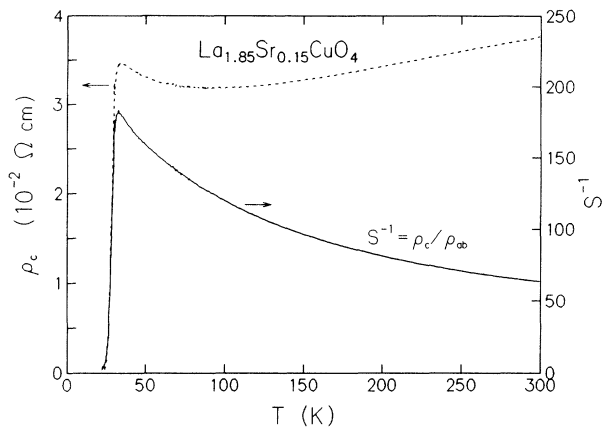


FIG. 6. Plots for $\rho_c(T)$ calculated from $\rho_{[010]}$ and $\rho_{[301]}$ (dashed line) and $S^{-1}(T) = \rho_c(T)/\rho_{ab}(T)$ (solid line), providing evidence for the abrupt decrease in the conductivity anisotropy in the transition region.

behavior of ρ_c in the transition region.

In the T range above 30 K, $S^{-1}(T)$ increases as T decreases. As indicated in Fig. 4, this leads to a greater underestimate of ρ at lower T , and then causes a substantially more positive curvature for $\rho(T)$, as seen in Fig. 1(c). More plainly, as the temperature decreases, S^{-1} increases and the current distribution becomes more inhomogeneous. Then the current flowing through a region covering the two voltage probes is reduced further and the voltage drop decreases further, too. Since the applied current is constant, the measured resistance is proportional to this voltage drop, as is the case in the usual measurements. Thus the increase in S^{-1} at lower temperatures apparently causes the very small resistivity and larger residual resistivity ratio.

Below 30 K, S^{-1} abruptly decreases. Then the current distribution becomes less inhomogeneous, and the voltage drop starts to become greater as T decreases. With further decrease in T , ρ_c and ρ_{ab} decrease substantially, and accordingly the voltage drop decreases to zero. Thus, as T decreases from above T_c , the voltage drop first increases and then decreases, showing a peak behavior. Thus, again, the present model sufficiently explains the RP behavior in Fig. 1(c).

IV. DISCUSSION

The present result has two implications. First, almost all the previous experimental results on the RP turn out to have a simple origin. They are definitively explained by the present model. It is easy to find the conditions that bring about the RP in those earlier studies. Some of them provide reinforcing evidence that the RP was seen only in samples that have a very high residual resistivity ratio.⁸ In those experiments, it is difficult to rule out the possibility that the as-grown crystal surfaces have a step structure, which is topologically identical to that shown in the inset of Fig. 4. Even if the crystal surface is parallel to the CuO_2 planes, the sample configuration seen in Ref. 2, for example, is also topologically identical to a bi-

crystal consisting of two crystals of the type shown in the inset of Fig. 4. Thus the present result provides a very different interpretation of the RP from those mentioned in Refs. 1 or 2.

The second implication concerns the difference between the behavior of the superconducting resistive transition in the c -axis direction and in the CuO_2 planes. The present results indicate that the resistive transition is much faster in its onset along the c axis than in the CuO_2 planes. The reasons for this can be viewed in two ways as follows.

The existence of a finite transition width may indicate spatial electronic inhomogeneity as an extrinsic origin. In this case, the nucleation of small superconducting regions dispersed throughout the sample drastically reduces the resistance along the c axis like pinhole shortcuts in layered materials, while the change in ρ_{ab} is relatively slow.¹⁴ This causes an abrupt decrease in the conductivity anisotropy S^{-1} in the transition region, resulting in the RP. In this case, the field and current dependence of the peak height is expected to be moderate. In the present experiments, the RP remains in the presence of a magnetic field of 8 T, though the width becomes larger and its shape changes slightly, indicating that the RP in the (103) $\text{La}_{1.85}\text{Sr}_{0.15}\text{CuO}_4$ epitaxial films is probably has this extrinsic origin.

Other than the extrinsic origin, the following intrinsic origin attracts much interest and is physically important. In high- T_c superconductors or any other highly anisotropic systems, superconductivity is characterized by two-dimensional superconducting sheets coupled by the Josephson effect. In such systems, the Kosterlitz-Thouless transition plays an important role in the CuO_2 planes,¹⁵ while Josephson coupling is the dominant effect along the c axis.¹⁶ In a T range below and close to T_c , ρ_{ab} remains at a finite value due to the thermal fluctuation of free vortices and antivortices. In this T range, ρ_{ab} decreases slowly until T decreases to the vortex-unbinding Kosterlitz-Thouless transition temperature. On the other hand, interlayer Josephson coupling sets in at T_c and ρ_c decreases by orders of magnitude, resulting in an abrupt decrease in the anisotropy.¹⁷ Then, similarly, the RP appears. This intrinsic origin is more sensitive to an applied magnetic field and current density, because the maximum Josephson current density is a sensitive function of field and current. If the probing current exceeds the maximum Josephson current, or a magnetic field is applied, ρ_c appears again and S^{-1} increases to a value comparable to that in a higher T range. Then the RP vanishes or decreases in height in the presence of a magnetic field or large current density, as pointed out in the case of $\text{Bi}_2\text{Sr}_2\text{CaCu}_2\text{O}_{8-y}$ (Ref. 2) and TaSe_3 (Ref. 8).

V. CONCLUSIONS

The RP near the resistive transition in high- T_c superconductors is definitively explained with a simple model.

The model requires very large anisotropy and a finite inclination of a sample face against the CuO_2 planes. In the resistivity measurements where these conditions are fulfilled, the usual four-probe method leads to serious underestimation of resistivity. Furthermore, in the resistive transition region, the RP appears due to the abrupt decrease in the conductivity anisotropy ratio. From this interpretation, it follows that the RP is a manifestation of the physical fact that the resistive transition along the c axis occurs much faster than in the CuO_2 planes.

ACKNOWLEDGMENTS

I have benefited from enlightening discussions with Professor N. Phuan Ong at Princeton University, Professor K. Kitazawa and T. Kimura at the University of Tokyo, Dr. Y. Ando and Dr. S. Tajima at ISTE, and Dr. S. Shamoto at Nagoya University. I am also grateful to Dr Y. Ishii and Dr. T. Edahiro for continued interest and encouragement and to Dr. M. Hikita, Dr. H. Asano, Dr. S. Kubo, Dr. K. Miyahara, and Dr. K. Tanabe for enlightening discussions.

-
- ¹M. A. Crusellas, J. Fontcuberta, and S. Piñol, *Phys. Rev. B* **46**, 14 089 (1992).
- ²Y. M. Wan, S. E. Hebboul, D. C. Harris, and J. C. Garland, *Phys. Rev. Lett.* **71**, 157 (1993).
- ³To the knowledge of the author, there is much unpublished data on the RP observed in crystals of high- T_c superconductors.
- ⁴N. Phuan Ong (private communication).
- ⁵K. Kitazawa and T. Kimura (private communication).
- ⁶S. Tajima and Y. Ando (private communication).
- ⁷Z. He, X. Cheng, J. Sha, Z. P. Su, Q. Zhang, J. Shi, and Z. Qi, *Solid State Commun.* **76**, 671 (1990).
- ⁸Y. Tajima and K. Yamaya, *J. Phys. Soc. Jpn.* **53**, 495 (1984); **53**, 3307 (1984); Y. Tajima, M. Morita, and K. Yamaya, *ibid.* **55**, 2121 (1986).
- ⁹R. Akihama and Y. Okamoto, *Solid State Commun.* **53**, 655 (1985).
- ¹⁰H. Yamamoto, M. Ikeda, and M. Tanaka, *Jpn. J. Appl. Phys.* **24**, L314 (1985).
- ¹¹For details, see M. Suzuki and T. Murakami, *Phase Transitions* **15**, 201 (1989); M. Suzuki, Y. Enomoto, and T. Murakami, in *Superconductivity*, edited by K. Kitazawa and K. Tachikawa, MRS International Proceedings No. 6 (Materials Research Society, Pittsburgh, 1989), p. 647; M. Suzuki and M. Hikita, *Phys. Rev. B* **41**, 9566 (1990). It should be noted that the occurrence of the RP indicates the absence of a mosaic structure in the 103 epitaxial films described here.
- ¹²T. Ito, H. Takagi, T. Ido, S. Ishibashi, and S. Uchida, *Nature* **350**, 69, (1991).
- ¹³M. Suzuki, *Phys. Rev. B* **39**, 2312 (1989).
- ¹⁴Consider a cube made of an anisotropic medium with edges of length L aligned in the basic directions, and, within the cube, a small cube (edge length l) as a nucleated superconducting region. Then the decreases in ρ_c is approximately $\rho_c l/L$, while that in ρ_{ab} is approximately $\rho_{ab} l^3/L^2(L-l)$.
- ¹⁵Y. Matsuda, S. Komiyama, T. Terashima, K. Shimura, and Y. Bando, *Phys. Rev. Lett.* **69**, 3228 (1992); L. C. Davis, M. R. Beasley, and D. J. Scalapino, *Phys. Rev. B* **42**, 99 (1990).
- ¹⁶R. Kleiner, F. Steinmeyer, G. Kunel, and P. Müller, *Phys. Rev. Lett.* **68**, 2394 (1992).
- ¹⁷This is also pointed out from a different point of view in Ref. 2 and by Y. M. Wan, S. E. Hebboul, D. C. Harris, and J. C. Garland, *Bull. Am. Phys. Soc.* **38**, 224 (1993); S. E. Hebboul, Y. M. Wan, D. C. Harris, and J. C. Garland, *ibid.* **38**, 224 (1993).

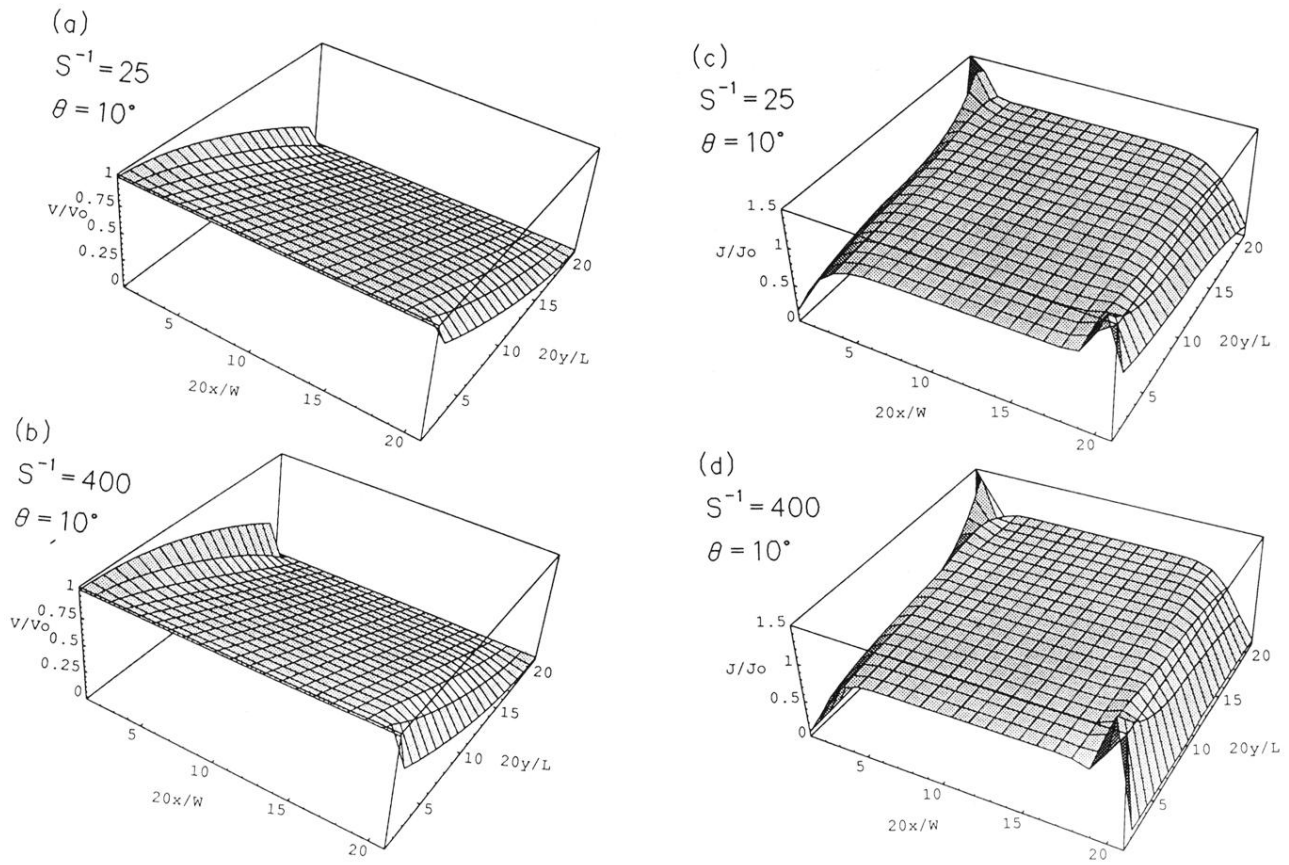


FIG. 3. Typical results of the numerical calculation of the potential $V(x,y)$ and current density distribution. (a) $V(x,y)/V$ when $S^{-1}=25$ and $\theta=10^\circ$, (b) $V(x,y)/V$ when $S^{-1}=400$ and $\theta=10^\circ$, (c) $J(x,y)$ when $S^{-1}=25$ and $\theta=10^\circ$, and (d) $J(x,y)$ when $S^{-1}=400$ and $\theta=10^\circ$. The values for $J(x,y)$ are normalized by the corresponding value when $\theta=0$.